THE JOURNAL OF BIOLOGICAL CHEMISTRY
Vol. 279, No. 35, Issue of August 27, pp. 36746–36752, 2004
Printed in U.S.A.

Overactive Bladder and Incontinence in the Absence of the BK Large Conductance Ca^{2+}-activated K^+ Channel*

Received for publication, May 20, 2004, and in revised form, June 2, 2004
Published, JBC Papers in Press, June 7, 2004, DOI 10.1074/jbc.M405621200

Andrea L. Meredith‡, Kevin S. Thorneloe§¶, Matthias E. Werner§, Mark T. Nelson§, and Richard W. Aldrich‡‖

From the ‡Department of Molecular and Cellular Physiology and the Howard Hughes Medical Institute, Stanford University, Stanford, California 94305 and the §Department of Pharmacology, University of Vermont, Burlington, Vermont 05405

BK large conductance voltage- and calcium-activated potassium channels respond to elevations in intracellular calcium and membrane potential depolarization, braking excitability of smooth muscle. BK channels are thought to have a particularly prominent role in urinary bladder smooth muscle function and therefore are candidate targets for overactive bladder therapy. To address the role of the BK channel in urinary bladder function, the gene *mSlo1* for the pore-forming subunit of the BK channel was deleted. *Slo*$^{-/-}$ mice were viable but exhibited moderate ataxia. Urinary bladder smooth muscle cells of *Slo*$^{-/-}$ mice lacked calcium- and voltage-activated BK currents, whereas local calcium transients ("calcium sparks") and voltage-dependent potassium currents were unaffected. In the absence of BK channels, urinary bladder spontaneous and nerve-evoked contractions were greatly enhanced. Consistent with increased urinary bladder contractility caused by the absence of BK currents, *Slo*$^{-/-}$ mice demonstrate a marked elevation in urination frequency. These results reveal a central role for BK channels in urinary bladder function and indicate that BK channel dysfunction leads to overactive bladder and urinary incontinence.

Overactive urinary bladder and urinary incontinence is a significant health issue occurring in about 51 million (~17%) of the United States population (1), frequently occurring as a secondary consequence of conditions such as diabetes mellitus, stroke, and spinal cord injury. Urge incontinence is caused by overactivity of the urinary bladder smooth muscle (UBSM),[1] often a result of partial urethral outlet obstruction that can occur during prostate hypertrophy. Currently there is a lack of effective therapeutic agents to control urinary bladder function. Antimuscarinic agents, which impair UBSM contraction, are used to treat urinary incontinence but have limited effectiveness and undesirable side effects. More recently, potassium channel opening drugs have been explored as therapeutic agents for urinary incontinence (2–6).

BK potassium channels regulate membrane potential and repolarization of UBSM action potentials (7–8). UBSM BK channels are activated by membrane potential depolarization and calcium influx through voltage-dependent calcium channels that occur during the action potential (9). UBSM BK channels are also activated by local intracellular calcium release through ryanodine receptors (calcium sparks) (10). Specific inhibition of BK channels by iberiotoxin (IBTX) causes a pronounced elevation in bladder contractility (8, 11–12). Deletion of the smooth muscle-specific, modulatory β1 subunit decreases the apparent voltage- and calcium-sensitivity of UBSM BK channels, leading to an enhancement of phasic contractility (12). These studies point to a pivotal role of the BK channel in urinary bladder function.

EXPERIMENTAL PROCEDURES

Generation of Slo$^{-/-}$ Mice—mSlo1 genomic clones were isolated from a 129/SvJ BAC library (Incyte Genomics) using an ~1.6-kb EcoRV/XhoI cDNA probe fragment. A 7.8-kb SalI/BamHI genomic fragment containing exon 1 was cloned into pPNT (13–14). Synthetic double-stranded oligos containing *loxP* recognition sequences for Cre recombinase were cloned 5′ (XhoI site, 5′-TCCCTCGAATAACTTCGTATAGCATACATTATACGAAGTTATTCGAGCCC-3′) and 3′ (NcoI site, 5′-GGATCCATAACTTCGTATAGCATACATTATACGAAGTTATCCATGG-3′) of exon 1. Enhanced green fluorescent protein containing β-globin basal promoter elements and a bovine growth hormone polyadenylation signal (a gift from Dr. Jane Johnson) was subcloned into the *mSlo1* intronic sequence at the NcoI site. For removal of the *neo* cassette, oligos containing FRT recognition sites for Flp recombinase were subcloned into the XhoI and XbaI sites flanking PGKneo (5′-CTCGATGAAGTTCCTATACTTTCTAGAGAATAGGAACTTCGGAATAGGAACTTCTCGAG-3′ and 5′-TCTAGGAAGTTCCTATACTTTCTAGAGAATAGGAACTTCGGAATAGGAACTTCAGATCC-3′). An ~1.2-kb BamHI/KpnI *mSlo1* genomic fragment was subcloned 3′ of the *neo* cassette into XbaI/KpnI of pPNT.

The targeting construct was linearized for transfection with NotI and electroporated into R1 embryonic stem cells. After ganciclovir and G418 selections, six correct integrants were identified by PCR. To verify intact integration of the entire targeting construct, these clones were analyzed by Southern blot using external 5′ and 3′ probes on XhoI and BamHI/MfeI-digested genomic DNA, respectively. Two correctly integrated clones were injected into C57Bl/6 blastocyst stage embryos, producing five germ line-transmitting founders.

To generate a whole animal *Slo*$^{-/-}$ mutant, founder males were crossed to FVB-TgN(EIIa-Cre)C5379Lmgd females (Jackson Laboratories), a line that ubiquitously expresses Cre from the adenoviral *EIIa* promoter. All F1 progeny had stable, germ line-transmissible deletions of exon 1, as confirmed by Southern blot analysis (Fig. 1*B*). Heterozygotes were backcrossed >6 generations to FVB/NJ. Intercrosses to obtain homozygous *Slo*$^{-/-}$ were genotyped by PCR on tail DNA.

PCR Genotyping of Slo$^{-/-}$ Mice—Tail snips were digested overnight at 55 °C in 750 μl of SNET (20 mM Tris, pH 8, 1 mM EDTA, 1% SDS, 0.4 M NaCl) plus 15 μl of 20 mg/ml proteinase K and extracted with an

* This work was supported by a National Institutes of Health grant (to M. T. N.) and by the Mathers Foundation (to R. W. A.). The costs of publication of this article were defrayed in part by the payment of page charges. This article must therefore be hereby marked "*advertisement*" in accordance with 18 U.S.C. Section 1734 solely to indicate this fact.

¶ Recipient of fellowships from the Canadian Institutes for Health Research and the Alberta Heritage Foundation for Medical Research.

‖ An investigator with the Howard Hughes Medical Institute. To whom correspondence should be addressed: Dept. of Molecular and Cellular Physiology and Howard Hughes Medical Institute, 279 Campus Dr., Beckman 173, Stanford University, Stanford, CA 94305. Tel.: 650-723-6531; Fax: 650-725-4463; E-mail: raldrich@stanford.edu.

[1] The abbreviations and trivial terms used are: UBSM, urinary bladder smooth muscle; BK, large conductance calcium-activated K^+ channel; IBTX, iberiotoxin; *Slo*$^{-/-}$, *mSlo1* homozygous null.

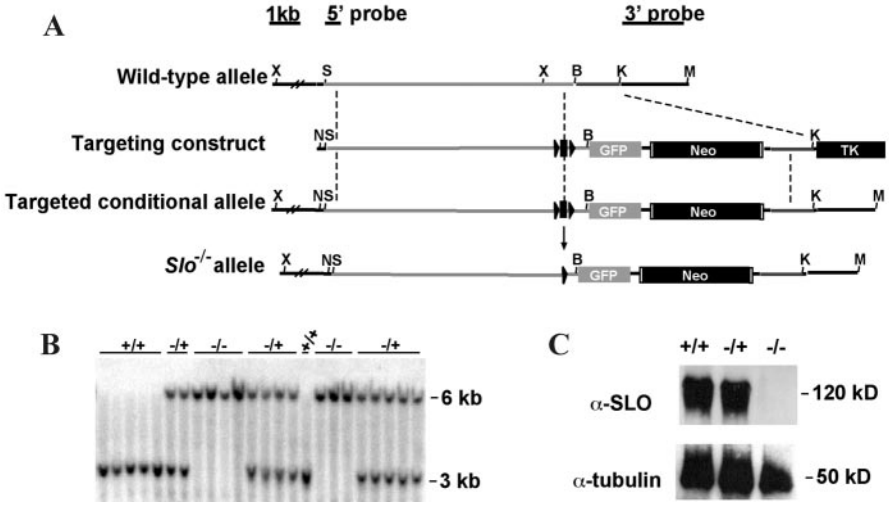

FIG. 1. **Generation of *Slo*$^{-/-}$ mice.** *A*, portion of wild-type (*Slo*$^{+/+}$) *mSlo1* genomic locus, targeting construct, targeted conditional allele containing the FRT-flanked *neo* cassette (*white boxes*), and the mutant (*Slo*$^{-/-}$) allele that has undergone Cre-mediated recombination deleting exon 1. The *black box* represents exon 1, flanked by *loxP* sites (*triangles*). *X*, XhoI; *S*, SalI; *B*, BamHI; *K*, KpnI; *M*, MfeI; *N*, NotI; *TK*, thymidine kinase; *GFP*, green fluorescent protein. *B*, Southern blot analysis of BamHI/MfeI-digested genomic tail DNA from two litters hybridized with the 3′ probe, *Slo*$^{-/-}$ allele 6 kb. *C*, Western blot analysis of bladder proteins probed with α-*Slo* and D1Mα α-tubulin antibodies.

equal volume 1:1 phenol/chloroform. DNA was ethanol-precipitated and 500 ng of DNA (or 2 μl of supernatant) was used in PCR reactions (NEB Taq, supplier's reaction condition plus 2% Me_2SO; amplification conditions: 94 °C, 2 min; (94 °C, 30 s; 55–50 °C, 30 s; 72 °C, 2 min) × 5 cycles; (94 °C, 30 s; 50 °C, 30 s; 72 °C, 2 min) × 30 cycles; 72 °C, 5′; 4 °C, hold). Neo 5′ (5′-ATA GCC TGA AGA ACG AGA TCA GC-3′) and RA 14025 3′ (5′-CCT CAA GAA GGG GAC TCT AAA C-3′) amplify the *Slo*$^{-/-}$ allele product of 800 bp. Exon 1 5′-3 (5′-TTC ATC ATC TTG CTC TGG CGG ACG-3′) and WT 3′-2 (5′-CCA TAG TCA CCA ATA GCC C-3′) amplify the wild-type product of 332 bp.

Isolation of UBSM and Western Blotting—All procedures involving mice were in accordance with Institutional Animal Care and Use Committee policies at the University of Vermont and Stanford University. *Slo*$^{+/+}$ and *Slo*$^{-/-}$ mice 1.5–3 months of age were sacrificed by intraperitoneal injection of a lethal dose of sodium pentobarbital (150 mg/kg) or CO_2 euthanasia.

For Western blots, urinary bladders were solubilized in lysis buffer (137 mM NaCl, 1% Triton X-100, 0.5% deoxycholate, 40 mM HEPES, pH 7.4, 1 mM EDTA, pH 7.4, 2 μg/ml aprotinin, 1 μg/ml leupeptin, 2 μg/ml antipain, 10 μg/ml benzamidine, and 0.5 mM phenylmethylsulfonyl fluoride). The insoluble fraction was separated by centrifugation (14,000 × *g* for 5 min). 5 μg of soluble supernatant protein (assayed by Bio-Rad DC protein assay reagent) underwent SDS-PAGE on a 7.5% acrylamide gel prior to being transferred to a nitrocellulose membrane. Membranes were blocked in 4% dry nonfat milk, 2% normal goat serum, 10 mM Tris (pH 8), 0.15 M NaCl, and 0.1% Tween 20 for 1 h. They were then labeled with primary antibodies in blocking solution overnight, 1:5000 each of rabbit polyclonal α-*Slo* (Alamone Labs, Jerusalem, Israel) and mouse monoclonal DM 1A α-tubulin (Sigma). Membranes were labeled with 1:500 SuperSignal West Dura horseradish peroxidase-conjugated goat α-rabbit and α-mouse secondary antibodies (Pierce), and proteins were visualized by SuperSignal chemiluminescence detection (Pierce).

Electrophysiology—UBSM cells from *Slo*$^{+/+}$ and *Slo*$^{-/-}$ mice were isolated enzymatically for perforated whole-cell patch clamp recordings at 22 °C as previously described (15–16). The bath and pipette solutions contained the following (mM): 134 NaCl, 6 KCl, $MgCl_2$, 2 $CaCl_2$, 10 glucose, and 10 Hepes, pH 7.4 (NaOH), and 110 potassium aspartate, 30 KCl, 10 NaCl, 1 $MgCl_2$, 0.05 EGTA, 200 μg ml^{-1} amphotericin B, and 10 Hepes, pH 7.2 (KOH), respectively. Iberiotoxin (Sigma) was used at a final concentration of 100 or 300 nM.

Ca^{2+} Spark Measurements—Isolated UBSM cells were loaded on glass coverslips with the Ca^{2+}-sensitive fluorophore, fluo 4-AM (Molecular Probes), in cell isolation solution (16) with 10 μM fluo 4-AM, 0.04% pluronic acid, and 2 mM $CaCl_2$ for 20 min. After loading, UBSM cells were washed with electrophysiology bath solution, and Ca^{2+} imaging was conducted on a laser-scanning confocal microscope (OZ; Noran Instruments) at room temperature, acquiring images at 120 or 30 Hz with scan durations of 25 s. Ca^{2+} sparks were defined as local increases in fluorescence of 1.3 F/F_o (F, instantaneous; F_o, baseline fluorescence) that persisted for at least two images and were analyzed with custom software written by Dr. Adrian Bonev using IDL Research Systems (17–19). F_o was obtained by averaging 10 images that displayed no Ca^{2+} sparks. For quantitation of Ca^{2+} sparks, a box (10 × 10 pixels, 2.2 × 2.2 μm) was placed over the Ca^{2+} spark site, and F/F_o traces were generated.

Contractility Studies—Contractility experiments were performed at 37 °C as previously described (20) using a MyoMed myograph system (MED Associates Inc.). Electrical field stimulation was at 20 Hz (20 V amplitude, alternating polarity between pulses, 0.2-ms stimulation width) delivered once a minute for 2 s. Electrical field stimulation evoked a robust contraction of UBSM strips that was completely blocked by 1 μM tetrodotoxin (n = 3). IBTX was dissolved in water and added directly to the bathing solution at a concentration of 100 nM. Spontaneous phasic contractile activity was analyzed using MiniAnalysis (Synaptosoft, Inc.).

Urination Patterns—Female mice 1–2.5 months of age were placed in standard cages for 1 h with the bedding replaced by Whatman Grade 3 filter paper. Food and water were given *ad libitum*. Urine spots were photographed under UV light (21–22).

Statistical Analyses—Results are expressed as means ± S.E. where applicable. Comparisons were made with the two-tailed Student's t test (before and after IBTX application were paired, *Slo*$^{+/+}$ *versus* *Slo*$^{-/-}$ were unpaired).

RESULTS

Generation of Slo$^{-/-}$ *Mice*—To test the hypothesis that BK channel dysfunction leads to overactive bladder and urinary incontinence, we created a targeted mutation of the pore-forming subunit, encoded by the *mSlo1* gene, by homologous recombination in embryonic stem cells using standard techniques (14). A conditional allele of the *mSlo1* gene was generated by flanking exon 1 with *loxP* sites, which enables deletion of exon 1 by expression of Cre recombinase (Fig. 1*A*). Exon 1 contains the translation start site as well as the S0 transmembrane segment of the channel necessary for formation of functional channels (23). Ubiquitous expression of Cre recombinase deletes exon 1, generating a stable, germ line-transmissible mutant allele (Fig. 1*B*, *Slo*$^{-/-}$). *mSlo1* transcripts (n = 3) and protein (Fig. 1*C*) are undetectable in UBSM from *Slo*$^{-/-}$ mice, indicating the allele is a null.

General Phenotypes of Slo$^{-/-}$ *Mice*—We examined the general features of *Slo*$^{-/-}$ mice using behavioral and histological analysis. Although *mSlo1* is widely expressed (24) and BK channels are postulated to be important in many tissues, *Slo*$^{-/-}$ mice exhibit grossly normal organ development (n = 5) and neurological signs (n = 10) (25). Although *Slo*$^{-/-}$ mice are born in approximately normal Mendelian ratios (Fig. 1*B*, 28.5% *Slo*$^{+/+}$, 50% *Slo*$^{+/-}$, and 21.5% *Slo*$^{-/-}$, n = 296 mice), they are 27% smaller than *Slo*$^{+/+}$ littermates (weight at 2 weeks: *Slo*$^{+/+}$, 9.2 ± 0.6 g, n = 8; *Slo*$^{-/+}$, 7.2 ± 0.2 g, n = 30; *Slo*$^{-/-}$, 6.7 ± 0.3 g, n = 13). However, by 5 weeks of age their body mass is similar to littermates (*Slo*$^{+/+}$, 19.5 ± 0.5 g, n = 15;

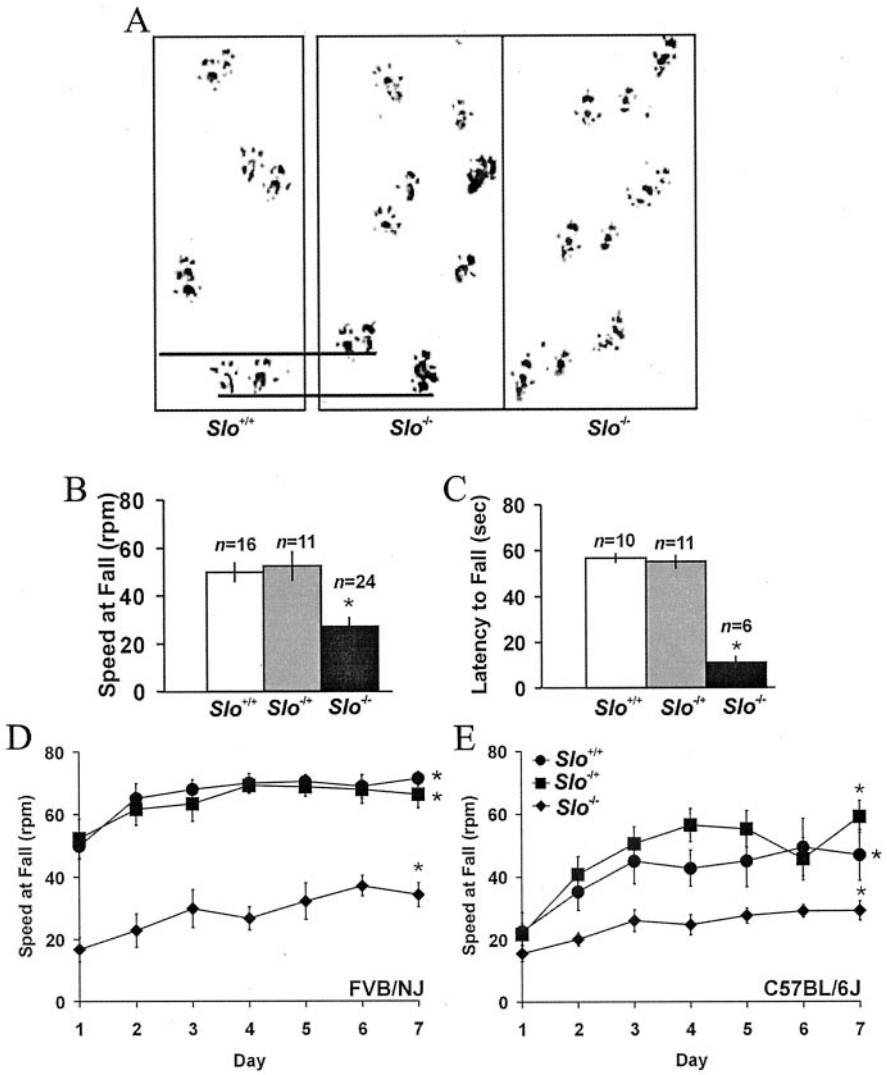

FIG. 2. ***Slo*$^{-/-}$ mice have ataxia and deficits in motor performance.** *A*, footprint patterns from representative *Slo*$^{+/+}$ and *Slo*$^{-/-}$ mice. Mouse feet were inked, and the mice were sent through a 35-cm tunnel to produce a straight running trajectory. Lines indicate the stride length (1.2 cm) for a *Slo*$^{-/-}$ mouse. *Slo*$^{-/+}$ mice produce a footprint pattern indistinguishable from *Slo*$^{+/+}$. *B*, rotarod assay. Mice were placed on an accelerating rod (13 rpm/min) to a maximum speed of 79 rpm. Plotted data are the average of two consecutive trials of the rotarod speed at which the mice fell. *C*, hanging wire assay. Mice were allowed to grasp the wire cage lid, and then the lid was slowly inverted to allow the mice to maintain their grasp for a 60-s trial. The data represent the average of two consecutive trials. *D* and *E*, rotarod learning assay. Using the same parameters as in *panel B*, the average of two trials was graphed for 7 consecutive days: *Slo*$^{+/+}$, *circles*, $n = 16$; *Slo*$^{-/+}$, *squares*, $n = 11$; *Slo*$^{-/-}$, *diamonds*, $n = 6$ (*D*). *, $p < 0.05$ Day 1 *versus* Day 7 for each genotype, indicating motor learning. All mice in the reported assays were >1 month old and on an inbred FVB/NJ background, except for *panel E*, which was on a mixed F2 C57BL/6J background (*Slo*$^{+/+}$, $n = 8$; *Slo*$^{-/+}$, $n = 9$; *Slo*$^{-/-}$, $n = 10$).

Slo$^{-/+}$, 19.4 ± 0.5 g, $n = 20$; *Slo*$^{-/-}$, 20.0 ± 0.9 g, $n = 7$). On an inbred FVB/NJ background, 40% of *Slo*$^{-/-}$ mice die at an average age of 2.2 ± 0.3 months of unknown causes ($n = 48$). The surviving mutant mice have apparently normal life spans (>10 months).

Surprisingly, *Slo*$^{-/-}$ mice are able to produce offspring. Although the efficiency of successful matings is significantly reduced, 1 of 20 *Slo*$^{-/-}$ males (set up for mating to wild-type females) was able to sire a litter of normal size (9 pups, $n = 1$ litter). Despite the proposed role of BK channels in uterine smooth muscle quiescence during pregnancy (26–27), *Slo*$^{-/-}$ females can carry litters to term and adequately feed and care for their pups (average litter sizes from females mated to *Slo*$^{+/-}$ males: *Slo*$^{+/-}$ mothers, 7.8 ± 0.4 pups, $n = 23$ litters; *Slo*$^{-/-}$ mothers, 3.9 ± 0.5 pups, $n = 7$ litters).

The pervasive phenotype demonstrated by all *Slo*$^{-/-}$ mice is moderate ataxia. Footprint analysis reveals that *Slo*$^{-/-}$ mice have a shorter stride length (Fig. 2*A*). The gait pattern of a 35-cm segment was analyzed for each mouse by inking their feet and running them through a straight tunnel on white paper (25). *Slo*$^{+/+}$ mice had an average stride length of 3.1 ± 0.1 cm ($n = 5$ mice), whereas *Slo*$^{-/-}$ mice displayed an uneven gait pattern with a stride length of 1.8 ± 0.1 cm ($n = 6$, $p < 0.05$). In a test of motor performance, *Slo*$^{-/-}$ mice fell off an accelerating rotarod at significantly slower speeds compared with littermates (Fig. 2*B*). However, motor learning is not impaired (Fig. 2, *D* and *E*). *Slo*$^{-/-}$ mice also perform poorly in the hanging wire assay (25), a task requiring grip strength as well as motor coordination for which mice grasp an inverted cage lid and the time period before falling is measured (Fig. 2*C*). Our data do not distinguish between deficits in central neurons (cerebellum, basal ganglia, vestibular, or motor), peripheral neurons (sensory), or skeletal muscle, but none of these tissues is abnormal by gross morphology or histological examination in Slo$^{-/-}$ mice ($n = 7$). The underlying cause of the ataxia is currently being investigated with tissue-specific Cre lines and the *Slo* conditional allele.

Interestingly, 6% of mutants also exhibit persistent spontaneous circling ($n = 47$). This unidirectional circling is likely because of a functional deficit; necropsies on affected *Slo*$^{-/-}$ mice did not reveal any cerebellar, basal ganglia, vestibular, or other lesions ($n = 2$).

Slo Encodes Voltage-activated, IBTX-sensitive K$^+$ *Currents in UBSM*—UBSM cells isolated from *Slo*$^{+/+}$ mice exhibit a pronounced BK channel current, measured as the voltage-activated outward current inhibited by IBTX, a selective blocker of BK channels (Fig. 3). BK channel currents are absent in UBSM cells from *Slo*$^{-/-}$ mice (Fig. 3).

We further examined the properties of UBSM cells isolated from *Slo*$^{+/+}$ and *Slo*$^{-/-}$ mice. The whole-cell capacitance was not different, indicating similar cell sizes (*Slo*$^{+/+}$ 40 ± 4 pF, $n = 17$; *Slo*$^{-/-}$ 47 ± 3 pA/pF, $n = 12$; $p > 0.05$). We assessed voltage-gated (IBTX-insensitive) K^+ currents using a depolarizing step protocol. Voltage-gated K^+ current densities were

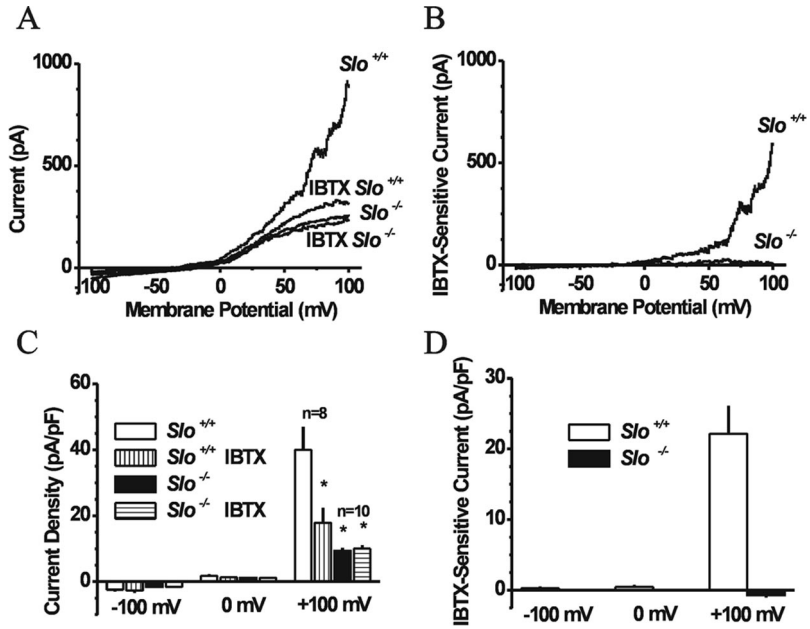

FIG. 3. **Absence of voltage-activated BK currents in $Slo^{-/-}$ UBSM cells.** *A*, whole-cell 800-ms depolarizing ramp currents ± iberiotoxin (*IBTX*) from freshly isolated $Slo^{+/+}$ and $Slo^{-/-}$ UBSM cells. *B*, IBTX-sensitive currents from $Slo^{+/+}$ and $Slo^{-/-}$ ramp recordings shown in *panel A*. *C* and *D*, average ramp current values at different voltages for *panels A* and *B*, respectively. *, significantly different from $Slo^{+/+}$ control, $p < 0.05$.

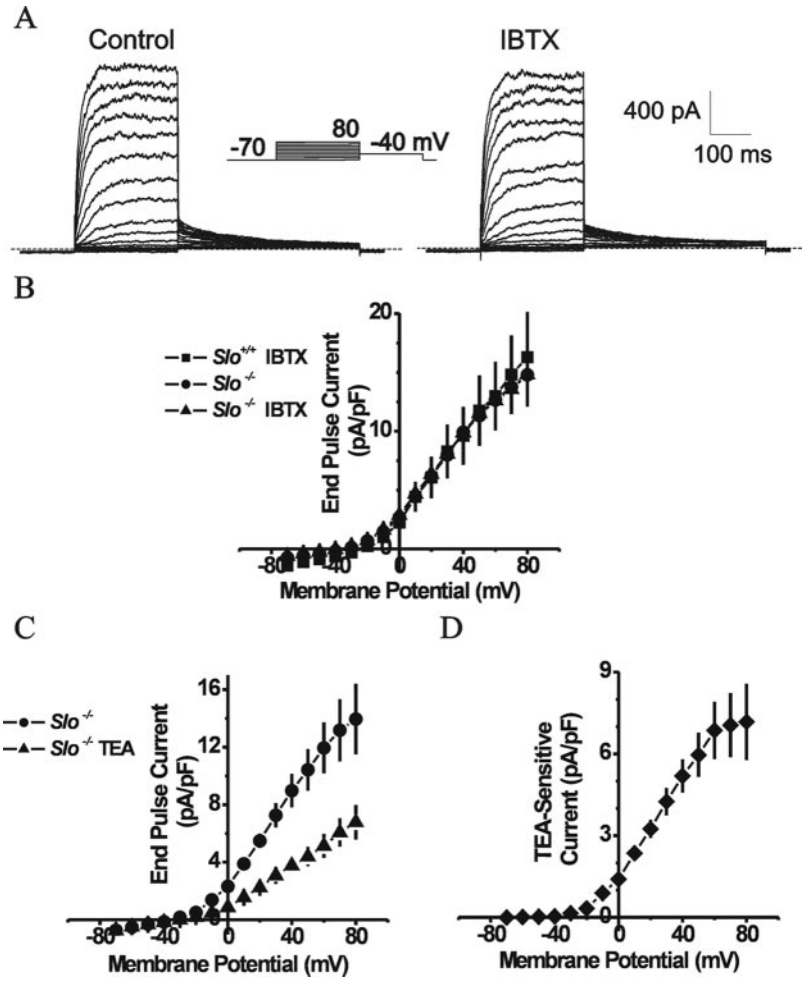

FIG. 4. **Voltage-gated potassium currents in $Slo^{-/-}$ UBSM cells.** *A*, representative whole-cell current from a $Slo^{-/-}$ UBSM cell plus and −IBTX, elicited by 250-ms depolarizing pulses (see *inset*). *B*, voltage-gated K^+ current density and current-voltage relationship for $Slo^{+/+}$ UBSM cells ($Slo^{+/+}$ *IBTX*, $n = 5$) is the same as for $Slo^{-/-}$ UBSM cells ($Slo^{-/-}$, $Slo^{-/-}$ *IBTX*, $n = 6$). *C*, voltage-gated K^+ current in $Slo^{-/-}$ UBSM cells is inhibited by 60% with 10 mM tetraethylammonium ion ($n = 4$). *D*, average tetraethylammonium ion-sensitive current density from $Slo^{-/-}$ UBSM cells ($n = 4$).

similar at all voltages (Fig. 4*B*). $Slo^{-/-}$ UBSM voltage-gated K^+ current was blocked by 60% with 10 mM tetraethylammonium ion (Fig. 4, *C* and *D*, *TEA*). These results are consistent with that reported for the mouse UBSM voltage-gated K^+ current (15).

Ca^{2+}-activated, Spontaneous Transient Outward Currents Are Absent in $Slo^{-/-}$ Mice—BK channels are activated by elevations in intracellular calcium and in particular by local and transient calcium release (calcium sparks) through ryanodine receptors in the sarcoplasmic reticulum membrane (9–10, 17, 28–30, 32). UBSM cells isolated from $Slo^{+/+}$ mice exhibit transient BK currents characteristic of those produced by calcium sparks. These are inhibited by 97% with IBTX (Fig. 5, *A* and *D*). Consistent with the lack of voltage-activated BK

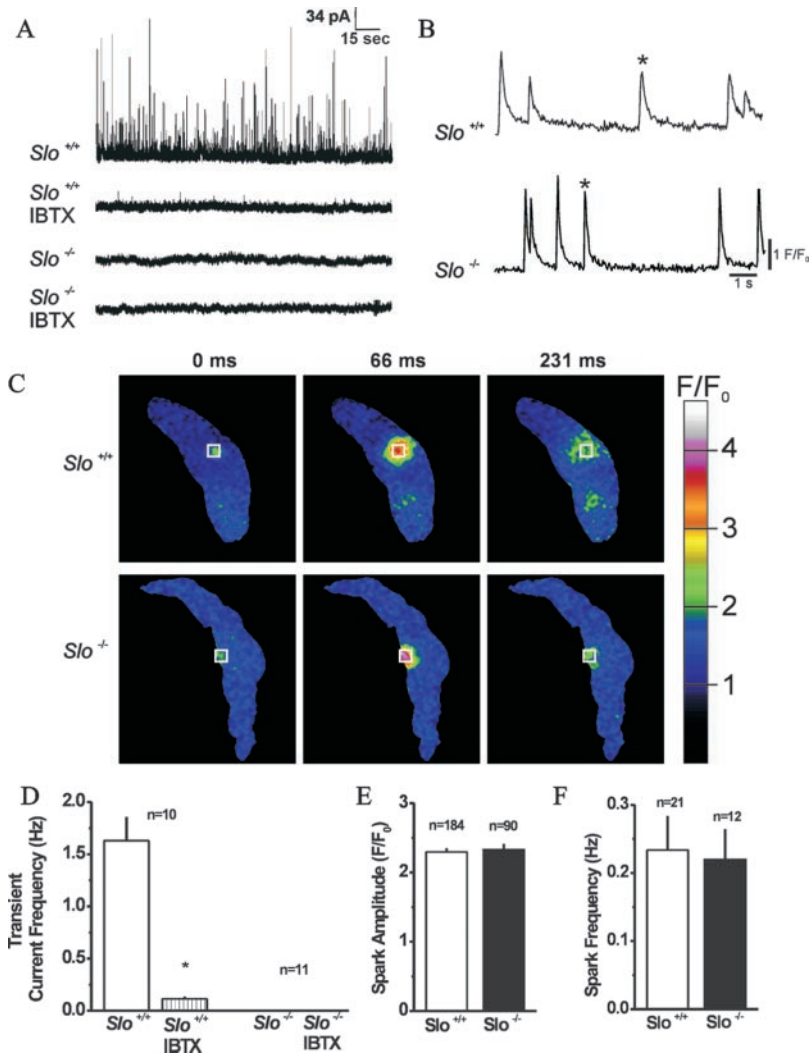

FIG. 5. **Absence of calcium-activated BK currents in *Slo*$^{-/-}$ UBSM cells with underlying local calcium transients (calcium sparks) unaltered.** *A*, transient Ca^{2+}-activated BK currents at 0 mV ± IBTX from UBSM cells. *B*, F/F_o (F, instantaneous; F_o, baseline fluorescence) *versus* time for calcium spark sites (*white boxes* in *panel C*, 2.2 × 2.2 μm) of UBSM cells. *C*, pseudocolor images of representative calcium sparks (indicated by * in *panel B*). F/F_o color scale, *right*. *D*, average transient BK current frequency from *panel A*. *E* and *F*, average calcium spark amplitude and frequency, respectively, were not different between *Slo*$^{+/+}$ and *Slo*$^{-/-}$ UBSM cells.

currents in UBSM cells of *Slo*$^{-/-}$ mice (Fig. 3), Ca^{2+}-activated transient BK currents were not detected in *Slo*$^{-/-}$ mice (Fig. 5, *A* and *D*). These data indicate that the *mSlo1* gene encodes the IBTX-sensitive BK channel activated by both voltage and calcium in UBSM.

A lack of transient BK currents in *Slo*$^{-/-}$ mice could reflect ryanodine receptor (calcium spark) dysfunction. However, calcium sparks were unchanged in *Slo*$^{-/-}$ mice. UBSM cells from *Slo*$^{+/+}$ and *Slo*$^{-/-}$ mice were loaded with the Ca^{2+}-sensitive indicator fluo-4, and changes in intracellular Ca^{2+} were monitored using a laser-scanning confocal microscope. We observed local transient increases in Ca^{2+} in UBSM cells from both *Slo*$^{+/+}$ and *Slo*$^{-/-}$ mice (Fig. 5, *B* and *C*), with spatial and temporal characteristics consistent with calcium sparks described previously (10, 17, 29, 30, 32). Furthermore, Ca^{2+} spark amplitude and frequency were not different between *Slo*$^{+/+}$ and *Slo*$^{-/-}$ UBSM cells (Fig. 5, *E* and *F*), and there were no differences in the number of spark sites/UBSM cell (*Slo*$^{+/+}$ 2.4 ± 0.5, n = 20; *Slo*$^{-/-}$ 2.4 ± 0.5, n = 12), Ca^{2+} spark duration (*Slo*$^{+/+}$ 186 ± 17 ms, n = 62; *Slo*$^{-/-}$ 172 ± 19 ms, n = 62), or in the decay of Ca^{2+} spark events (time constants: *Slo*$^{+/+}$ 138 ± 16 ms, n = 62; *Slo*$^{-/-}$ 128 ± 18 ms, n = 62).

Slo$^{-/-}$ *Demonstrate Enhanced UBSM Contractility Leading to Urinary Incontinence*—We next addressed the functional role of BK channels in urinary bladder contractility utilizing isolated UBSM strips. UBSM strips exhibit spontaneous phasic contractions that are important for the maintenance of urinary bladder tone and, when enhanced, likely contribute to overactive bladder (31). Phasic contraction area, amplitude, and frequency were increased in *Slo*$^{-/-}$ over *Slo*$^{+/+}$ mice (Fig. 6, *A–C*). Overall phasic contractile activity (frequency × area) was increased 4-fold in *Slo*$^{-/-}$ compared with *Slo*$^{+/+}$ mice.

Urine voiding (micturition) is caused by stimulation of parasympathetic nerves in the bladder wall. To explore the role of BK channels in nerve-mediated urinary bladder contraction, we utilized electrical field stimulation at a physiological frequency to selectively evoke neurotransmitter release in UBSM strips, thereby mimicking the excitation that occurs during micturition. Blocking BK channels with IBTX in *Slo*$^{+/+}$ UBSM strips resulted in a 40% enhancement of nerve-mediated contractions, an effect that was absent in *Slo*$^{-/-}$ strips (Fig. 6, *D* and *E*). Nerve-mediated contractions of UBSM strips from *Slo*$^{-/-}$ mice were significantly greater than the force produced by *Slo*$^{+/+}$ strips (Fig. 6, *D* and *F*). However, the contractile force elicited during membrane potential depolarization by elevating bathing (K^+) to 60 mM was not different between *Slo*$^{+/+}$ (5.7 ± 1.0 mN, n = 8) and *Slo*$^{-/-}$ strips (5.3 ± 0.9 mN, n = 8). Normalizing the nerve-mediated force to the K^+-induced force in each UBSM strip indicated a 3-fold increase in nerve-mediated contractions in *Slo*$^{-/-}$ UBSM (Fig. 6*G*). Therefore, in addition to increased phasic contractility in *Slo*$^{-/-}$ mice (Fig. 6, *A–C*), nerve-mediated contractions are also dramatically enhanced when BK channels are absent (Fig. 6, *D–G*).

The expression of BK channels in UBSM and the robust increase in UBSM contractility demonstrated by *Slo*$^{-/-}$ mice suggest that BK channels may be critical for normal bladder

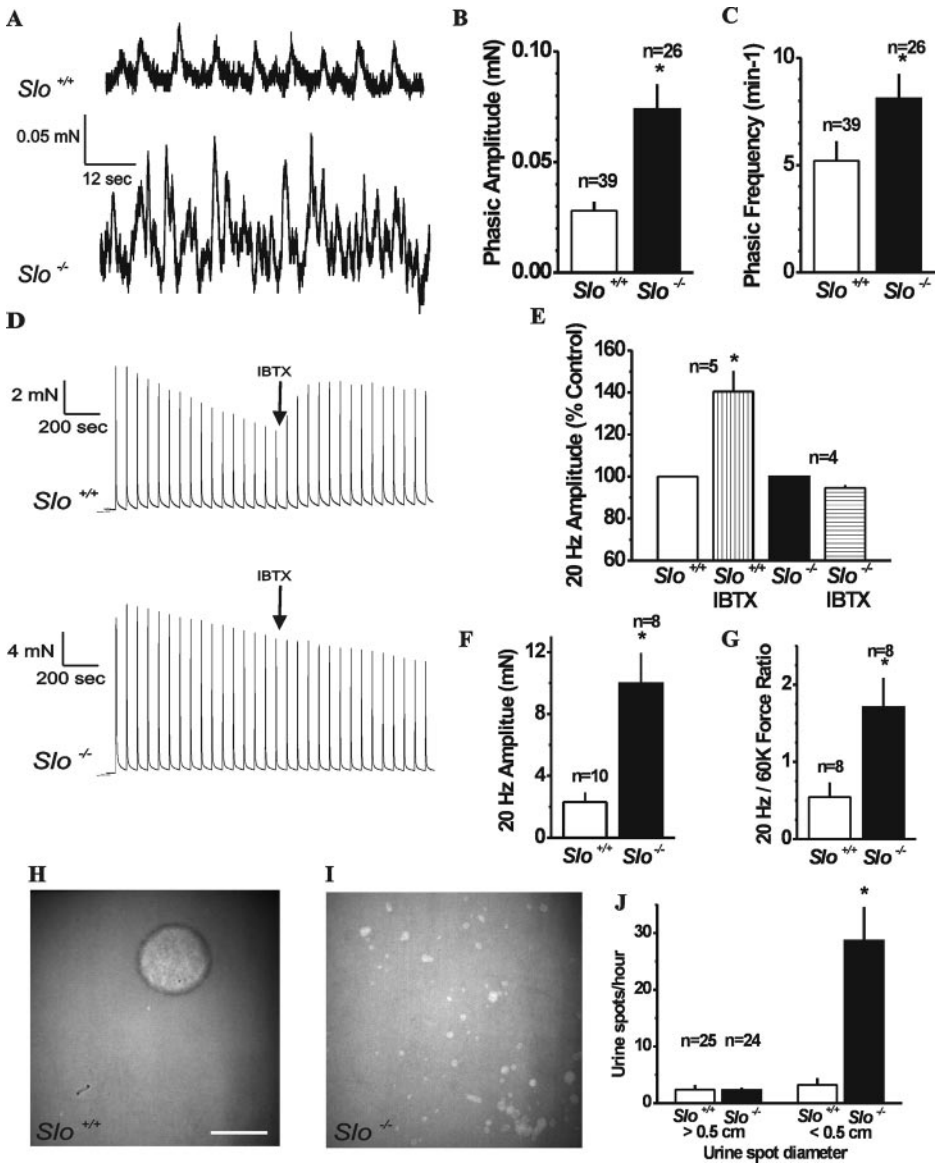

FIG. 6. **UBSM contractility and urination frequency is increased in *Slo*$^{-/-}$ mice.** *A*, representative phasic contractions recorded from UBSM strips. *B* and *C*, average amplitude and frequency, respectively, of phasic contractions shown in *panel A* (*n*, number of UBSM strips from 6 *Slo*$^{+/+}$ and 4 *Slo*$^{-/-}$ mice). *D*, representative nerve-mediated contractions from UBSM strips ± IBTX. *E*, average IBTX effect on nerve-mediated contractions. *F*, average electrical field stimulation-induced contraction amplitude from UBSM strips. *G*, amplitudes from *panel F* normalized to 60 mM K^+-induced contractions of each UBSM strip. *H* and *I*, representative urination pattern of freely moving female mice visualized on filter papers under UV light (*bar*, 2 cm). *Slo*$^{+/+}$ mouse produced one large spot (*H*), and *Slo*$^{-/-}$ mouse produced many small spots (*I*). *J*, average number and size distribution of urine spots quantified from filter papers (*, $p < 0.05$).

function *in vivo*. To test for urinary bladder overactivity in the absence of BK channels, the urination patterns of freely moving female *Slo*$^{+/+}$ and *Slo*$^{-/-}$ mice were assessed. *Slo*$^{+/+}$ mice produced an average of 2.4 ± 0.8-large diameter urine spots (>0.5 cm) in an hour, not significantly different from *Slo*$^{-/-}$ mice (Fig. *6, H–J,* 2.3 ± 0.4). However, *Slo*$^{-/-}$ mice produced 8.8 times more small urine spots (<0.5 cm) than *Slo*$^{+/+}$ mice. Additionally, *Slo*$^{-/-}$ mice exhibited yellow perineal staining ($n = 10$), which was absent in *Slo*$^{+/+}$ littermate controls ($n = 10$). No significant differences in water intake (*Slo*$^{+/+}$ 3.3 ± 0.1 ml/day, $n = 5$; *Slo*$^{-/-}$ 3.2 ± 0.3 ml/day, $n = 10$) or urine production, measured as urine-specific gravity (*Slo*$^{+/+}$ 1.058 ± 0.006, $n = 9$; *Slo*$^{-/-}$ 1.072 ± 0.003, $n = 7$), were observed that could account for the increased urination frequency observed in *Slo*$^{-/-}$ mice. This suggests that the overactivity in *Slo*$^{-/-}$ bladders is not a result of increased urine production by the kidneys but is a functional deficit in the urinary bladder itself caused by the absence of BK channels.

DISCUSSION

In this study, we have demonstrated that the absence of functional BK currents (Figs. 3–5) significantly enhances basal and nerve-mediated UBSM contractility (Fig. 6, *A–G*), leading to bladder overactivity and urinary incontinence (Fig. 6, *H–J*). BK channels normally activate in response to depolarization and increases in intracellular Ca^{2+} during UBSM action potentials, thereby limiting excitability and contractility. Without this feedback pathway, as in *Slo*$^{-/-}$ mice, excitability remains unchecked, leading to detrusor muscle instability, a primary cause of urinary incontinence.

Currently, the underlying basis of human bladder detrusor instability is not well understood, and its etiology likely involves a number of interrelated factors. Our study suggests that BK channels could be a potent therapeutic target for both neurologic and myogenic causes of bladder dysfunction. The increased frequency of spontaneous contractions in *Slo*$^{-/-}$ mice suggests that enhancing feedback modulation by potentiating BK channels in patients with underlying myogenic causes for incontinence could alleviate bladder overactivity. Similarly, the increased force of contractions in response to a voiding stimulus in UBSM of *Slo*$^{-/-}$ mice suggests that individuals with neurologically caused incontinence would also benefit from BK channel augmentation. Consistent with this idea, delivery of *hSlo1* cDNA into rat urinary bladder decreased bladder overactivity caused by partial urethral outlet obstruction (31). Thus, the development of selective BK channel activators (3, 5–6) may be an effective therapy for the variety of

bladder overactivity dysfunctions observed in patient populations, without the undesirable side effects of existing autonomic antagonists. Finally, these novel results provide definitive evidence that BK channel dysfunction can lead to overactive bladder and urinary incontinence.

Acknowledgments—We thank Luke Baxter for assistance with mouse ataxia behavior experiments, Jason Phillips for genotyping and RT-PCR, and Dr. Donna Bouley for necropsy expertise.

REFERENCES

1. Hu, T. W., Wagner, T. H., Bentkover, J. D., Leblanc, K., Zhou, S. Z., and Hunt, T. (2004) *Urology* **63**, 461–465
2. Li, J. H., Yasay, G. D., Zografos, P., Kau, S. T., Ohnmacht, C. J., Russell, K., Empfield, J. R., Brown, F. J., Trainor, D. A., Bonev, A. D., Heppner, T. J., and Nelson, M. T. (1995) *Pharmacology* **51**, 33–42
3. Butera, J. A., Antane, S. A., Hirth, B., Lennox, J. R., Sheldon, J. H., Norton, N. W., Warga, D., and Argentieri, T. M. (2001) *Bioorg. Med. Chem. Lett.* **11**, 2093–2097
4. Brune, M. E., Fey, T. A., Brioni, J. D., Sullivan, J. P., Williams, M., Carroll, W. A., Coghlan, M. J., and Gopalakrishnan, M. (2002) *J. Pharmacol. Exp. Ther.* **303**, 387–394
5. Hewawasam, P., Erway, M., Thalody, G., Weiner, H., Boissard, C. G., Gribkoff, V. K., Meanwell, N. A., Lodge, N., and Starrett, J. E., Jr. (2002) *Bioorg. Med. Chem. Lett*. **12**, 1117–1120
6. Turner, S. C., Carroll, W. A., White, T. K., Gopalakrishnan, M., Coghlan, M. J., Shieh, C. C., Zhang, X. F., Parihar, A. S., Buckner, S. A., Milicic, I., and Sullivan, J. P. (2003) *Bioorg. Med. Chem. Lett.* **13**, 2003–2007
7. Heppner, T. J., Bonev, A. D., and Nelson, M.T. (1997) *Am. J. Physiol.* **273**, C110-117
8. Hashitani, H., and Brading, A. F. (2003) *Br. J. Pharmacol.* **140**, 159–169
9. Herrera, G. M., and Nelson, M. T. (2002) *J. Physiol*. **541**, 483–492
10. Herrera, G. M., Heppner, T. J., and Nelson, M. T. (2001) *Am. J. Physiol*. **280**, C481–C490
11. Herrera, G. M., Heppner, T. J., and Nelson, M. T. (2000) *Am. J. Physiol.* **279**, R60–R68
12. Petkov, G. V., Bonev, A. D., Heppner, T. J., Brenner, R., Aldrich, R. W., and Nelson, M. T. (2001) *J. Physiol.* **537**, 443–452
13. Tybulewicz, V. L., Crawford, C. E., Jackson, P. K., Bronson, R. T., and Mulligan, R. C. (1991) *Cell* **65,** 1153–1163
14. Joyner, A. L. (1993) *Gene Targeting: A Practical Approach,* pp. 1–61 and 107–146, Oxford University Press, Oxford
15. Thorneloe, K. S., and Nelson, M. T. (2003) *J. Physiol.* **549**, 65–74
16. Horn, R., and Marty, A. (1988) *J. Gen. Physiol.* **92**, 145–159
17. Perez, G. J., Bonev, A. D., Patlak, J. B., and Nelson, M. T. (1999) *J. Gen. Physiol.* **113**, 229–238
18. Jaggar, J. H., and Nelson, M. T. (2000) *Am. J. Physiol.* **279**, C1528-C1539
19. Wellman, G. C., Santana, L. F., Bonev, A. D., and Nelson, M. T. (2001) *Am. J. Physiol.* **281**, C1029–C1037
20. Herrera, G. M., Pozo, M. J., Zvara, P., Petkov, G. V., Bond, C. T., Adelman, J. P., and Nelson, M. T. (2003) *J. Physiol*. **551**, 893–903
21. Thor, K. B., Blais, D. P., and de Groat, W. C. (1989) *Dev. Brain Res.* **46**, 137–144
22. Birder, L. A., Nakamura, Y., Kiss, S., Nealen, M. L., Barrick, S., Kanai, A. J., Wang, E., Ruiz, G., De Groat, W. C., Apodaca, G., Watkins, S., and Caterina, M. J. (2002) *Nat. Neurosci*. **5**, 856–860
23. Wallner, M., Meera, P., and Toro, L. (1996) *Proc. Natl. Acad. Sci. U. S. A.* **93**, 14922–14927
24. Sah, P., and Faber, E. S. (2002) *Prog. Neurobiol.* **66,** 345–353
25. Crawley, J. N. (2000) *What's Wrong with My Mouse? Behavioral Phenotyping of Transgenic and Knockout Mice,* pp. 31–63 and 120–122, Wiley-Liss, New York
26. Anwer, K., Oberti, C., Perez, G. J., Perez-Reyes, N., McDougall, J. K., Monga, M., Sanborn, B. M., Stefani, E., and Toro, L. (1993) *Am. J. Physiol.* **265,** C976-C985
27. Song, M., Zhu, N., Olcese, R., Barila, B., Toro, L., and Stefani, E. (1999) *FEBS. Lett.* **460,** 427–432
28. Nelson, M. T., Cheng, H., Rubart, M., Santana, L. F., Bonev, A. D., Knot, H. J., and Lederer, W. J. (1995) *Science* **270**, 633–637
29. Imaizumi, Y., Torii, Y., Ohi, Y., Nagano, N., Atsuki, K., Yamamura, H., Muraki, K., Watanabe, M., and Bolton, T. B. (1998) *J. Physiol.* **510**, 705–719
30. Imaizumi, Y., Henmi, S., Uyama, Y., Atsuki, K., Torii, Y., Ohizumi, Y., and Watanabe, M. (1996) *Am. J. Physiol.* **271**, C772–C782
31. Christ, G. J., Day, N. S., Day, M., Santizo, C., Zhao, W., Sclafani, T., Zinman, J., Hsieh, K., Venkateswarlu, K., Valcic, M., and Melman, A. (2001) *Am. J. Physiol.* **281**, R1699–R1709
32. Ohi, Y., Yamamura, H., Nagano, N., Ohya, S., Muraki, K., Watanabe, M., and Imaizumi, Y. (2001) *J. Physiol.* **534**, 313–326

Overactive Bladder and Incontinence in the Absence of the BK Large Conductance Ca^{2+}-activated K^{+} Channel

Andrea L. Meredith, Kevin S. Thorneloe, Matthias E. Werner, Mark T. Nelson and Richard W. Aldrich

J. Biol. Chem. 2004, 279:36746-36752.
doi: 10.1074/jbc.M405621200 originally published online June 7, 2004
